Biosensors and Bioelectronics 81 (2016) 159–165

Contents lists available at ScienceDirect

Biosensors and Bioelectronics

journal homepage: www.elsevier.com/locate/bios

Sensitive and rapid detection of aflatoxin M1 in milk utilizing enhanced SPR and p(HEMA) brushes

Aleksandra Karczmarczyk [a,c,*], Monika Dubiak-Szepietowska [a], Mariia Vorobii [d], Cesar Rodriguez-Emmenegger [d,e], Jakub Dostálek [b], Karl-Heinz Feller [a]

[a] Department of Medical Engineering and Biotechnology, Ernst-Abbe-University of Applied Sciences Jena, Carl-Zeiss Promenade 2, 07745 Jena, Germany
[b] BioSensors Technologies, AIT Austrian Institute of Technologies GmbH, Muthgasse 11, 1190 Wien, Austria
[c] Institute of Analytical Chemistry, University of Regensburg, Josef-Engert Straße, 93053 Regensburg, Germany
[d] Institute of Macromolecular Chemistry, Academy of Sciences of the Czech Republic, Heyrovsky Sq. 2, 16206 Prague, Czech Republic
[e] DWI – Leibniz Institute for Interactive Materials and Institute of Technical and Macromolecular Chemistry, RWTH Aachen University, Forckenbeckstraße 50, 52074 Aachen, Germany

ARTICLE INFO

Article history:
Received 20 January 2016
Received in revised form
22 February 2016
Accepted 23 February 2016
Available online 24 February 2016

Keywords:
Surface plasmon resonance
Aflatoxin
Polymer brushes
Gold nanoparticles
Inhibition immunoassay
Signal amplification

ABSTRACT

The rapid and sensitive detection of aflatoxin M_1 (AFM_1) in milk by using surface plasmon resonance (SPR) biosensor is reported. This low molecular weight mycotoxin is analyzed using an indirect competitive immunoassay that is amplified by secondary antibodies conjugated with Au nanoparticles. In order to prevent fouling on the sensor surface by the constituents present in analyzed milk samples, an interface with poly(2-hydroxyethyl methacrylate) p(HEMA) brush was employed. The study presents a comparison of performance characteristics of p(HEMA)-based sensor with a regularly used polyethylene glycol-based architecture relying on mixed thiol self-assembled monolayer. Both sensors are characterized in terms of surface mass density of immobilized AFM_1 conjugate as well as affinity bound primary and secondary antibodies. The efficiency of the amplification strategy based on Au nanoparticle is discussed. The biosensor allowed for highly sensitive detection of AFM_1 in milk with a limit of detection (LOD) as low as 18 pg mL^{-1} with the analysis time of 55 min.

1. Introduction

Aflatoxins are a family of extremely toxic and carcinogenic secondary metabolites (mycotoxins) secreted by certain species of *Aspergillus*. In particular, *Aspergillus flavus*, *Aspergillus parasiticus* and *Aspergillus nominus* contaminate a large variety of food and feed commodities (Creppy, 2002). Aflatoxin M_1 (AFM_1) is the hydroxylated derivative of aflatoxin B_1 (AFB_1) originating from the activity of cytochrome P450-associated enzyme in liver. It is excreted into the milk of both human and animals that have been fed with AFB_1 polluted diet (Polychronaki et al., 2007; Fallah, 2010). About 0.3–6.2% of AFB_1 in animal feed is transformed to AFM_1 in milk (Unusan, 2006). This compound elicits a wide spectrum of toxicological and carcinogenic effects causing liver cirrhosis, tumors or liver damage of human as well as animals (Canton et al., 1975; Deshpande, 2002; Zhang et al., 2013). The International Agency for Research on Cancer (IARC) recently reconsidered its carcinogenicity categorization, initially classified as a Group 2B human carcinogen, and changed it to Group 1 (Lyon, 2014). Despite the fact that milk and dairy products, such as cheese and yogurt are an important source of many essential nutrients like proteins, magnesium, calcium or vitamins B12 and A, unfortunately, they are also the most potent providers of AFM_1 among foods. Due to the relative stability during heat treatments (*e.g.* pasteurization) and significant threat to human health, especially to children who are the major consumers of milk, many countries have implemented regulations to control the content of AFM_1 in daily products (Galvano et al., 1996). The European Commission stipulates a maximum permissible level of 50 ng L^{-1} for AFM_1 in milk and dried or processed milk products (Regulation, 2006). In China and United States the regulations mandate AFM_1 levels below 500 ng L^{-1} (US Food and Drug Administration, 1996).

Sampling and analysis of mycotoxins are regulated by the European Commission Directives. The stipulated methods include high performance liquid chromatography with fluorimetric detection (HPLC-FD) coupled with the pre-cleaning by immunoaffinity columns (IF) (Radoi et al., 2008). This procedure

* Corresponding author at: Department of Medical Engineering and Biotechnology, Ernst-Abbe-University of Applied Sciences Jena, Carl-Zeiss Promenade 2, 07745 Jena, Germany.

http://dx.doi.org/10.1016/j.bios.2016.02.061
0956-5663/

relies on extensive sample preparation and the analysis requires couple of hours. Other, currently performed, techniques such as thin-layer chromatography (TLC) (Sassahara et al., 2005; Kamkar, 2006) or enzyme-linked immunosorbent assay (ELISA) (Pe et al., 2009) are also time consuming and require highly trained personnel, expensive equipment deployed in specialized laboratories. In order to simplify the analysis of mycotoxins, research is carried out to provide faster and sensitive techniques suitable for routine assay of milk and other dairy products. Over the last years we witnessed efforts to expedite AFM_1 detection based on immunoassays combined with fluorescence (Sapsford et al., 2006), electrochemistry (Micheli et al., 2005), colorimetry (Garden and Strachan, 2001) or chemiluminescence (Magliulo et al., 2005) readout.

A promising alternative to fluorescence assays are label-free biosensors based on surface plasmon resonance (SPR) (Homola, 2008). This technology exploits the measurement of changes in the reflective index occurring upon the affinity binding of molecules in the proximity of a metallic surface. As the response of SPR sensor is proportional to the mass of target molecule, direct detection of small molecules, such as mycotoxins, and/or analytes at very low concentration is challenging. Therefore, alternative assay formats are required for mycotoxin detection by using SPR. In order to enhance the sensor response, it was utilized a competition for binding to the surface between an antigen conjugated with a high molecular weight label and the unlabeled sample antigen. An alternative way is to immobilized the same molecule —antigen— which will be measured to the sensor surface, followed by injection of the primary antibodies and sample containing free antigen mixture. In this latter case, the signal can be further amplified by using the secondary antibodies labeled with metallic nanoparticles (NPs), magnetic nanoparticles (MNPs), fluorophores or quantum dots (QDs) (Wang et al., 2009, 2011; Campione and Capolino, 2011; Hu et al., 2014). Recently, several studies have reported the signal amplification by the implementation of gold nanoparticles (AuNPs). It can be designed to harness several effects including enhanced surface area, refractive index changes by the particles mass, and electromagnetic field coupling between the plasmonic properties of the particles and propagating plasmons (Mitchell et al., 2005; Szunerits et al., 2014).

Another challenging aspect in SPR analysis of complex samples such as milk and dairy products is the non-specific interaction at the surface that is associated with the deposition of non-targeted molecules or entities. SPR biosensors require an interface design for anchoring specific bioreceptors that is at the same time resistant to non-specific adsorption (Rodriguez-Emmenegger et al., 2011). To overcome the problem with fouling, different strategies of surface modification were proposed: grafting of carboxymethyl dextran (O'Shannessy et al., 1992), passivation with albumin (Homola et al., 2002) or a relatively new, however, very promising modification with various types of non-fouling polymer brushes. Such surface architecture has been shown to provide significantly higher fouling suppression (Vaisocherová et al., 2008; Rodriguez-Emmenegger et al., 2011; Kuzmyn et al., 2014; de los Santos Pereira et al., 2015), demonstrating their applications in a real-world biosensing (Vaisocherová et al., 2009; Brault et al., 2010; Rodriguez-Emmenegger et al., 2011; Hu et al., 2014). Considering milk analysis, it has been reported remarkably ultra-low fouling properties of antibody functionalized poly(2-hydroxyethyl methacrylate) p(HEMA) for the direct detection of *Cronobacter* in milk (Rodriguez-Emmenegger et al., 2011).

In this work, we describe an SPR biosensing for rapid, sensitive and specific detection of low molecular weight analyte AFM_1 in complex milk samples. The resistance to non-specific adsorption from milk was assessed by using the p(HEMA) brushes and the assay performance was compared to recent state-of-the-art antifouling polyethylene glycol (PEG) moieties. An indirect competitive immunoassay was developed for the analysis of low molecular analyte and the amplification of the sensor response by using secondary antibodies with metallic nanoparticles labels.

2. Materials and methods

2.1. Reagents

All reagents were used as received without further purification. Dithiol PEG6-COOH and dithiol PEG3-OH were purchased from SensoPath Technologies. 1-ethyl-3-(3-dimethylaminopropyl) carbodiimide hydrochloride (EDC) and *N*-hydroxysuccinimide (NHS) were obtained from Pierce (USA). *N*,*N*-dimethylformamide (DMF, 99.8%), 4-(dimethylamino) pyridine (DMAP), *N*,*N*'-disuccinimidyl carbonate (DSC), aflatoxin M_1 (AFM_1), the conjugate of AFM_1 with bovine serum albumin ($BSA–AFM_1$), PBS buffer tablets and Tween 20 were from Sigma-Aldrich. The primary rabbit antibody against AFM_1 (Ab_1) was from AntiProt and gold nanoparticles (AuNPs, 20 nm)-labeled goat anti-rabbit secondary antibody ($Ab_2–AuNPs$) from Abcam. The experiments were performed in PBS-Tween buffer (PBS-T) (pH 7.4) prepared by adding Tween 20 (0.05%) in PBS buffer solution. 20 mM acetate buffer (ACT, pH 4) was prepared from sodium acetate trihydrate and acetic acid (both from Sigma-Aldrich) and the pH was adjusted by HCl and NaOH. Glycine buffer with pH 1.5 and ethanolamine were purchased from Biocore (Germany). The ERM (European Reference Material) BD282 (zero level of AFM_1) was obtained from the Institute for Reference Materials and Measurements (Belgium).

2.2. Optical setup

An optical SPR biosensor setup utilizing angular spectroscopy of surface plasmons (SPs) was used. A transverse magnetically (TM) polarized beam with a wavelength of $\lambda = 632.8$ nm emitted from a HeNe laser (2 mW) was coupled to a right angle LASFN9 glass prism. To the prism base, a sensor chip was optically matched by using immersion oil. The sensor chip was prepared on the top of a BK7 glass substrate that was coated by sputtering (UNIVEX 450C form Leybold, Germany) with 41 nm thick gold layer. Then, the gold surface was either modified by a bicomponent SAM of thiols or polymer brushes for subsequent covalent immobilization of $BSA–AFM_1$ conjugates. A transparent flow-cell with a volume of approximately 10 μL was pressed against the surface of the sensor chip in order to flow liquid samples over the sensor surface by using a peristaltic pump at a flow rate of 500 μL min^{-1}. The intensity of the laser beam reflected from the sensor surface was measured using a photodiode detector. The resonant coupling to the SP is manifested as a resonance dip in the angular reflectivity spectrum $R(\theta)$. The binding of molecules to the gold layer was observed as a shift in the reflectivity dip, $\Delta\theta$, and evaluated by fitting with a transfer matrix-based model implemented in the software Winspall (developed at the Max Planck Institute for Polymer Research in Mainz, Germany). The whole sensor system and the supporting electronics were controlled by using the customized software Wasplas.

Since the refractive index is a linear function of concentration over a wide range of concentrations, the absolute amount of biomolecules bound at the surface (Γ) can be calculated using Feijter's formula (De Feijter et al., 1978):

$$\Gamma = \frac{(n_h - n_b)d_h}{\partial n/\partial c} \quad (1)$$

where n_h and n_b are the refractive indices of a protein monolayer ($n_h = 1.5$) and a buffer, respectively. The factor of $\partial n/\partial c = 0.18$ cm^3 g^{-1}

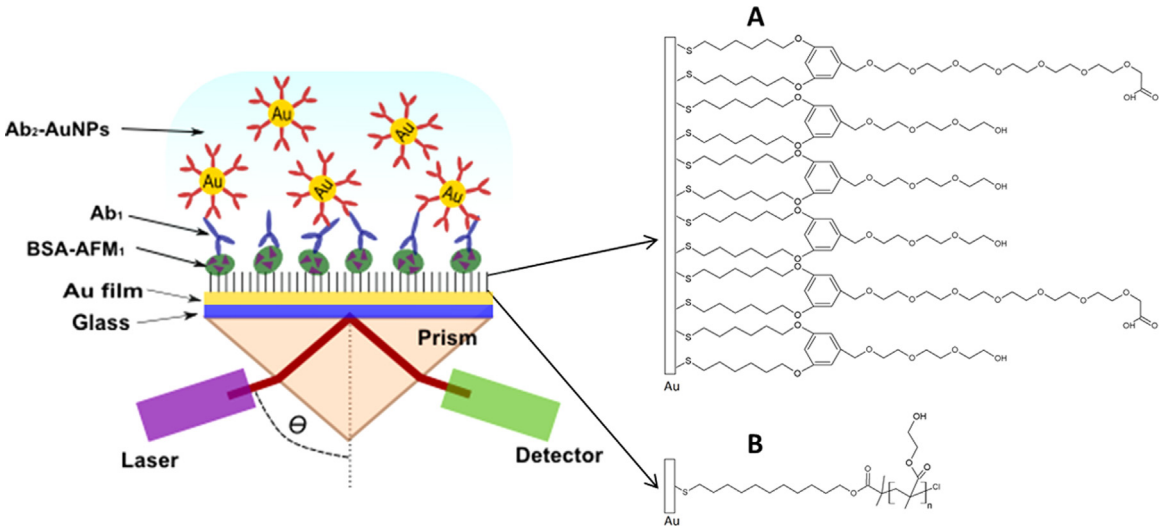

Fig. 1. The scheme of the optical setup and sensor chip with different surface architecture (A) mixed SAM and p(HEMA) brushes (B).

relates to the refractive index changes with the concentration of molecules and it was obtained from the literature (Kozma et al., 2011). The thickness of a layer d_h where the biomolecular binding occurs was determined by fitting the respective SPR spectrum using the following parameters: refractive index of the prism $n_p = 1.845$, complex refractive index for the gold film $n_m = 0.22 + 3.67i$, refractive index of the PBS-T buffer $n_b = 1.3337$.

2.3. Preparation of the chip surface

As Fig. 1 shows, two surface architectures were used for the attachment of AFM_1–BSA conjugate. The first (A) was based on a bicomponent SAM with PEG moieties and the second (B) utilized p(HEMA) polymer brushes. The thiol SAM was formed by overnight incubation of a gold surface at room temperature in a mixture of carboxyl-terminated and PEG-terminated dithiols (molar ratio 1:9) dissolved in ethanol at a total concentration of 1 mM. Subsequently, the sensor surface was rinsed with ethanol and dried in a stream of nitrogen. Afterwards, BSA–AFM_1 conjugate was *in situ* immobilized by using standard amine coupling chemistry. First, the carboxylic terminal groups were activated with a solution of EDC and NHS (concentrations in deionized water of 37.5 and 10.5 mg mL^{-1}, respectively) for 7 min. Afterward, a 40 μg mL^{-1} solution of BSA–AFM_1 conjugate in ACT buffer was circulated through the flow cell for 15 min to react *via* their amine groups with the sensor surface. The unreacted active ester groups were then blocked by 10 min incubation in 1 M ethanolamine at pH 8.5.

Polymer brushes of 2-hydroxyethyl methacrylate p(HEMA) were polymerized from a SAM of ω-mercaptoundecyl bromoisobutyrate on gold as described elsewhere (Rodriguez-Emmenegger et al., 2011). Briefly, p(HEMA) brushes were grown using a solution of $CuBr_2$, 2,2′dipyridyl, HEMA and CuCl in a mixture of water: ethanol 1:1 as a solvent (for the advancing and receding water contact angles measurement as well as FTIR-GASR spectra of p(HEMA) brushes, see Supplementary material). Brushes with thickness of 23.0 ± 0.3 nm were used for further experiments. Hydroxyl groups in p(HEMA) brushes were activated with a solution of DSC and DMAP (26 and 12 mg mL^{-1}, respectively, in anhydrous DMF) overnight at room temperature. Afterwards, the chips were rinsed with dry DMF, deionized water, blow dried with nitrogen and plugged to the SPR flow cell. BSA–AFM_1 conjugate was pumped through the flow cell and subsequently, unreacted groups reacted with ethanolamine.

2.4. Immunoassay procedure

For the detection of AFM_1, an inhibition immunoassay was carried out. PBS-T buffer or milk was spiked with AFM_1 at concentrations ranging from 10^{-1} to 10^3 ng mL^{-1}. These samples were prepared by sequential diluting of AFM_1 stock solution (concentration of 10 μg mL^{-1} in PBS buffer). The ERM-BD282 milk powder was dissolved in deionized water at the concentration of 0.1 g mL^{-1}. Then, samples containing AFM_1 were centrifuged at 5000 rpm for 20 min at the temperature of 4 °C. The upper fat layer was completely removed, and the obtained aqueous phase was directly used for the further analysis.

The analyzed sample was pre-incubated with Ab_1 antibody (concentration of 70 ng mL^{-1}) for 30 min. The mixture of sample and Ab_1 was flowed through the sensor for 10 min in order to allow the unreacted free Ab_1 to bind the BSA − AFM_1 conjugate immobilized on the surface. Subsequently, the sensor surface was washed with PBS-T buffer for 2 min to remove weakly bound Ab_1 molecules. Afterward, the Ab_2–AuNPs antibody (concentration of 0.1 μg mL^{-1}) was circulated through the sensor for 10 min, followed by 2 min rinsing with PBS-T. After each detection cycle, the sensor surface was regenerated by 5 min incubation in glycine buffer (pH 1.5, 20 mM) followed by rinsing with sodium hydroxide (20 mM).

3. Results and discussion

3.1. Affinity binding at thiol SAM and p(HEMA) brush architectures

SPR was used for the *in situ* observation of the covalent immobilization of BSA–AFM_1 and the subsequent affinity binding of Ab_1 and Ab_2–AuNPs. SPR reflectivity curves $R(\theta)$ were recorded for gold surface modified with thiol SAM and p(HEMA)-based brush, surfaces with immobilized BSA–AFM_1 conjugate, and after its affinity reaction with primary antibody Ab_1 and secondary antibody Ab_2 conjugated with AuNPs. On the chip modified by a mixed thiol SAM with PEG moieties, the resonant excitation of SPs occurs at $\theta = 57.1°$ which is manifested as a dip in the reflectivity spectrum $R(\theta)$, see Fig. 2A. In the case of chips functionalized with p(HEMA) brushes, this resonance is observed at higher angle of $\theta = 58°$ (Fig. 2B) as a consequence of the higher thickness. Upon the binding of biomolecules to the sensor surface, the surface mass density Γ increases which leads to a shift in SPR angle θ. As seen in

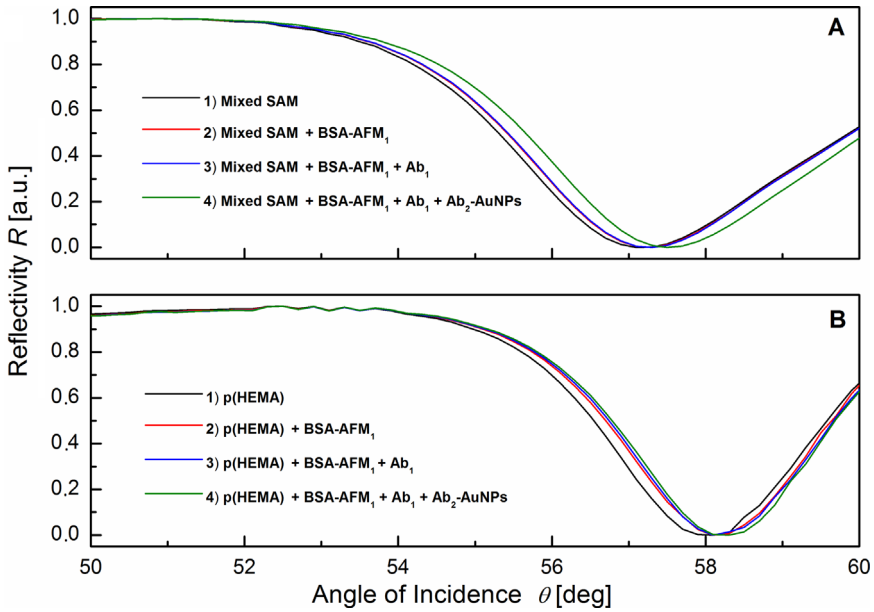

Fig. 2. Angular reflectivity spectra measured from a sensor chip for mixed SAM (A) and p(HEMA) brushes (B) prior the modification (1, only thiols SAM), after the immobilization of BSA–AFM_1 conjugate (2), and after affinity binding of Ab_1 (3) and Ab_2–AuNPs (4). The spectra were measured for the surface brought in contact with buffer.

Fig. 2, after the covalent functionalization with BSA–AFM_1 conjugate the resonant angle shift $\Delta\theta=0.11^\circ$ and $\Delta\theta=0.14^\circ$ for the PEG-SAM and p(HEMA) brush, respectively. By using Eq. (1), the corresponding surface mass density of BSA–AFM_1 was estimated to be $\Gamma=1.6$ ng mm^{-2} on the mixed SAM. The analysis of the reflectivity curves in Fig. 2B shows that a bare p(HEMA) brushes exhibit the thickness of 23 nm and refractive index of n_h=1.4714. These data correspond to a surface mass density of $\Gamma=17.5$ ng mm^{-2}. After the immobilization of BSA–AFM_1 in p(HEMA) brushes the surface mass density increases to 20.3 ng mm^{-2} indicating that the net surface mass density of coupled BSA–AFM_1 is 2.8 ng mm^{-2}. Afterward, the affinity binding of Ab_1 was tested for both tested architectures. Obtained results reveal a small shift of $\Delta\theta\approx0.02^\circ$ corresponding to $\Gamma\approx0.16$ ng mm^{-2}. Although, the molecular weight of IgG antibody is about 2.2 times higher than BSA–AMF_1, the surface mass density is significantly lower. The low concentration of the primary antibody Ab_1, short incubation time for which the binding may not reached the saturation and lack of antigen exposed for binding are among the feasible reasons for the low Ab_1 binding. Nevertheless, a very strong amplification of the sensor response $\Delta\theta$ was obtained by the subsequent reaction of the captured Ab_1 with Ab_2–AuNPs. An order of magnitude higher shift of $\Delta\theta=0.23^\circ$ was measured for the mixed SAM and lower shift $\Delta\theta=0.13^\circ$ was recorded for p(HEMA) architectures. This indicates that the affinity binding of large objects such as AuNPs decorated with Ab_2 to BSA–AFM_1 conjugate is partially hindered by the surrounding brush polymer chains. In order to check for the specificity of the interaction of Ab_1 and Ab_2 conjugated with AuNPs, the previous experiment was repeated for a sensor chip with immobilized BSA that was not conjugated with AFM_1. Not measurable response was observed after the flow of either Ab_1or Ab_2–AuNPs antibodies (data not shown).

The obtained results are in a good agreement with previous studies which showed that the immobilization density strongly depends on the surface density of hydroxyl groups (Rodriguez-Emmenegger et al., 2011). In a mixed SAM only carboxylic end groups can participate in the binding process, while in the case of p(HEMA) brushes, only the external layer of brushes with high density of functional groups provided by the polymer chain takes part in immobilization resulting in a similar range of functionalization (Trmcic-Cvitas et al., 2009).

3.2. Resistance to fouling from milk

Milk is a complex biological fluid composed of constituents including whey proteins (particularly β-lactoglobulin), lipids and calcium phosphate, which are involved in the fouling process through interacting mechanisms (denaturation, aggregation, local supersaturation) (Rosmaninho et al., 2007). The used surface architectures were exposed to the prepared standard milk samples and compared. As seen in the measured data in Fig. 3, these observations were made in real time and SPR changes were measured for an angle of incidence θ fixed at the resonance edge where the highest slope $\Delta R/\Delta\theta$ is occurs. The angle of incidence was set to $\theta=56.7^\circ$ and $\theta=57.3^\circ$ for mixed SAM and p(HEMA), respectively.

After obtaining a stable baseline in PBS-T, a milk sample was circulated over the sensor for *ca* 10 min, followed by 2 min washing with buffer. The amount of deposited material, fouling, was quantified as the difference in the resonance signal measured before and after the injection. As shown in Fig. 3, non-specific adsorption of components from milk is clearly visible on commonly used thiol SAMs with PEG moieties (Fig. 3B). Contrary to these results, excellent resistance to the non-specific interactions is observed for the sensor coated with p(HEMA) brush (Fig. 3A). After the washing step the reflectivity change is negligible. The sensitivity of SPR to fouling is more than 1 order of magnitude smaller than the fouling recorded in SAMs. According to previous studies, this phenomenon might be due to a water barrier resulting in minimization of hydrophobic effect with the lipids components form milk as well as to entropic barrier resulting from the brush architecture (Rodriguez-Emmenegger et al., 2011).

3.3. Aflatoxin M_1 detection

SPR technique offers the possibility to measure interactions in a real-time with high sensitivity and without the need of labels. Despite of many advantages arising from this method, its use for the analysis of small antigens (M_w < 1 kDa) or an analyte at low

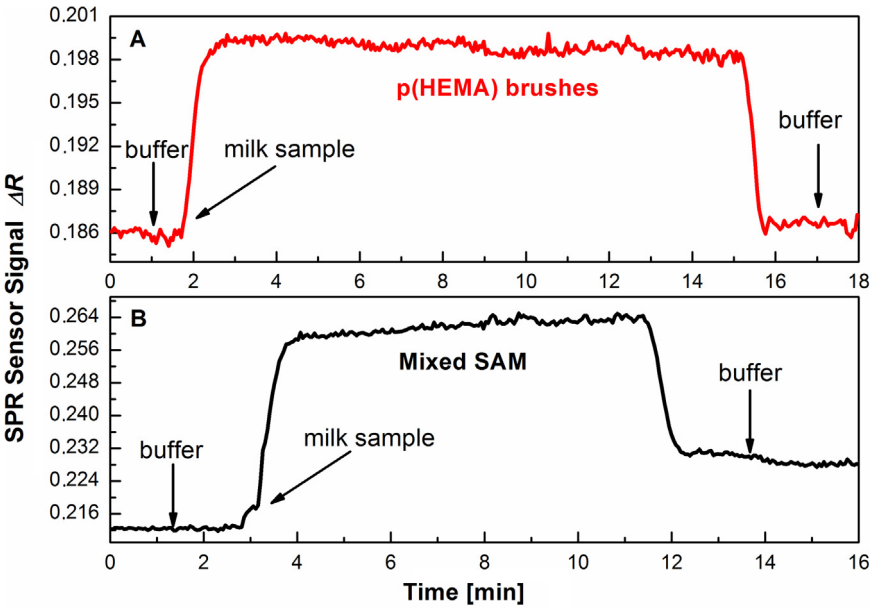

Fig. 3. Sensorgrams showing the differences in the SPR resonance signal recorded before and after injection of a milk sample (followed by washing with PBS-T buffer) on a chip coated with p(HEMA) brushes, revealing resistance to the non-specific interactions (A) and on mixed SAM, demonstrating adsorption of milk components (B).

concentration still poses challenges. When analytes with low M_w are detected, the resulting low mass of captured protein at the sensor surface is not sufficient to generate a detectable response by SPR. To increase the assay sensitivity, high-mass molecules or noble metal labels are required. In order to push the limit of detection of AFM_1 to concentrations stipulated by regulatory bodies, a competitive assay format was applied and the mass provided by the binding of primary antibodies Ab_1 was amplified by secondary antibodies Ab_2 labeled with gold nanoparticles AuNPs. The signal enhancement by employing AuNPs is caused not only by the size of NPs but also by the electromagnetic field coupling between localized surface plasmons of the nanoparticle and propagating plasmon field of the surface (Szunerits et al., 2014). Moreover, gold nanoparticles concentrate a high mass into a small volume and their surface allows convenient formation of coordinate bonds with thiols functional groups and so they can be easily conjugated to biomolecules as signal enhancement labels. When Ab_2–AuNPs conjugate solution was flowed over a chip with already captured Ab_1, the SPR response dramatically increased, demonstrating a 5-fold enhancement of the signal (data not shown). The sensor response was evaluated as the difference in the reflectivity ΔR before and after the assay cycle for series AFM_1 concentrations. Fig. 4 shows the obtained calibration curves normalized with the sensor response ΔR_0 measured in the absence of AFM_1 for the above-mentioned assay format. For each concentration, the sensor response ΔR was measured in triplicate and the standard deviation (SD) is indicated further as an error bar. The calibration curves were fitted with a sigmoidal function and the limit of detection (LOD) was determined as the concentration of AFM_1 which correspond to a sensor output equal to three standard deviation of the sensor output for the non-spiked liquids (blank samples). As seen in Fig. 4, the reflectivity change ΔR decreases with the increasing AFM_1 concentration due to the blocking of Ab_1 binding sites resulting in its lowest surface mass density at the sensor surface with AFM_1 conjugate.

The LOD for a sensor with thiol mixed SAM with PEG moieties was determined as 26 pg mL^{-1} and 38 pg mL^{-1} for the buffer and milk samples, respectively. The difference between LOD can be ascribed to the non-specific adsorption of milk constituents to the surface resulting in higher background response and deteriorated

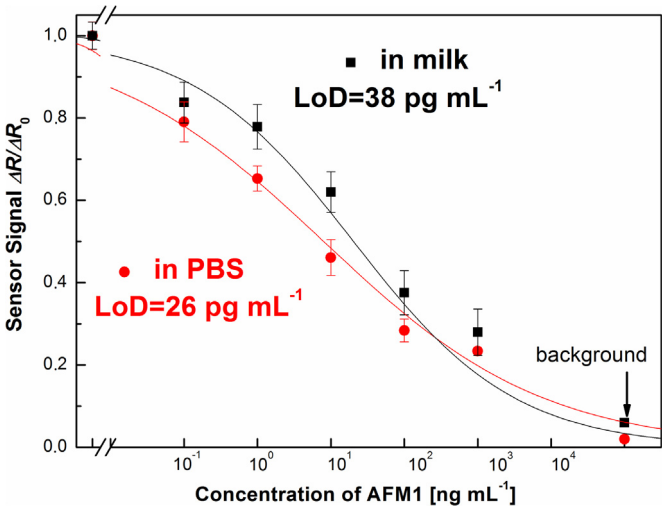

Fig. 4. Normalized calibration curves for the detection of AFM_1 using inhibition immunoassay on mixed SAM performed in a buffer (red circles) and milk (black squares). (For interpretation of the references to color in this figure legend, the reader is referred to the web version of this article.)

reproducibility. The coefficient of variation (CV) of the standard points of the calibration curves calculated for an assay performed in a buffer solution was in the range of 5–6% and 9–11% for experiments carried out in milk.

In order to reduce fouling from the milk samples, the assay was performed on the surface modified with p(HEMA) brush moieties. Fig. 5 shows a comparison of calibration curves obtained for two studied surface architectures. LOD of the sensor with p(HEMA) was determined as 18 pg mL^{-1} which is more than two-times lower compared to that on thiol SAM with PEG groups. The improvement of the LOD can be attributed to the elimination of the non-specific adsorption to the surface. This concomitantly, leaded to better reproducibility and excellent precision (the average calculated CV was below 4%) represented by error bars and lower background signal.

Compared to the performance of the other reported methods for the detection of aflatoxin M_1 in milk and milk products including

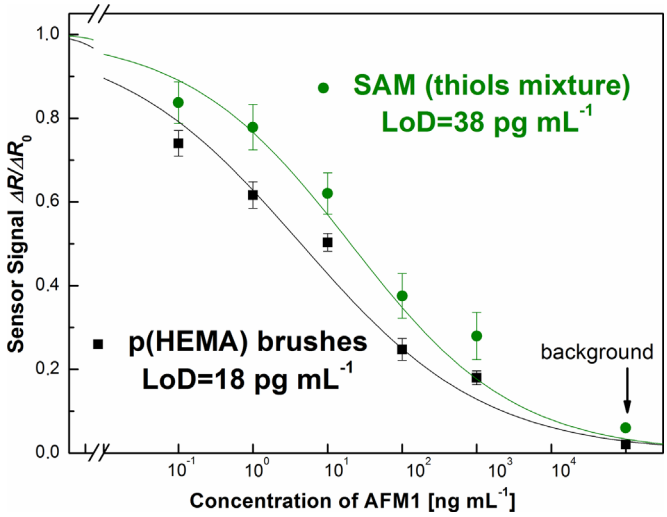

Fig. 5. Comparison of normalized calibration curves for the detection of AFM_1 in milk on the sensor surface coated with p(HEMA) brushes (black squares) and mixed SAM (green circles). (For interpretation of the references to color in this figure legend, the reader is referred to the web version of this article.)

electrochemistry (Micheli et al., 2005; Dinçkaya et al., 2011) or indirect and direct ELISA (Thirumala-Devi et al., 2002; Anfossi et al., 2008; Radoi et al., 2008) the presented biosensor provides about one order of magnitude higher sensitivity. Regarding the chemiluminescent technique reported by Magliulo et al. (2005) or LSPR detection described by Wang et al. (2009) where the obtained LOD was lower, the presently developed sensor offers shorter analysis time (*ca.* 55 min) and permits the detection of AFM_1 without compensation for the fouling. Nevertheless, the LOD of the developed biosensor can be further reduced by increasing the number of AFM_1 per BSA molecules, increasing the size of the gold nanoparticles and the time could be decreased by implementation of microfluidics, where smaller volume of the samples would reduce the time as well as improve the efficiency of binding.

4. Conclusions

A novel and highly sensitive SPR biosensor for AFM_1 analysis in milk was developed using inhibition assay format that allowed for the detection of toxin of interest at pg mL^{-1} levels. The limit of the detection was one order of magnitude lower than the maximum permissible level required by the European Commission. Modification of a gold chip surface with p(HEMA) showed excellent specificity and complete resistance to non-specific interaction, fouling. This is the first time that an SPR chip modified with such polymer brushes was used for real time detection of a small target antigen (AFM_1) utilizing indirect competitive immunoassay with AuNPs in milk samples. SPR-based sensors for small molecules suffer from high LOD due to high concentration of Ab_1 being needed to generate a sufficient signal. The current study shows that a combination of SPR and AuNPs enables signal enhancement and sensitivity improvement. Furthermore, such a system uses cheap reagents (Ab_2 and AuNPs) and significantly reduces the concentration of valuable Ab_1.

Acknowledgment

This work was supported by the Initial Training Network, SAMOSS, funded by the FP7 Marie Curie Actions of the European Commission (FP7-PEOPLE-2013-ITN) and by the Grant Agency of the Czech Republic (GACR) under Contract no. 15-09368Y.

Appendix A. Supplementary material

Supplementary data associated with this article can be found in the online version at http://dx.doi.org/10.1016/j.bios.2016.02.061.

References

Anfossi, L., Calderara, M., Baggiani, C., Giovannoli, C., Arletti, E., Giraudi, G., 2008. Development and application of solvent-free extraction for the detection of aflatoxin M1 in dairy products by enzyme immunoassay. J. Agric. Food Chem. 56 (6), 1852–1857.
Brault, N.D., Gao, C., Xue, H., Piliarik, M., Homola, J., Jiang, S., Yu, Q., 2010. Ultra-low fouling and functionalizable zwitterionic coatings grafted onto SiO_2 via a biomimetic adhesive group for sensing and detection in complex media. Biosens. Bioelectron. 25 (10), 2276–2282.
Campione, S., Capolino, F., 2011. Linear and planar periodic arrays of metallic nanospheres: fabrication, optical properties and applications. World Sci., 141–194.
Canton, J.H., Kroes, R., van Logten, M.J., van Schothorst, M., Stavenuiter, J.F.C., Verhülsdonk, C.A.H., 1975. The carcinogenicity of aflatoxin M1in rainbow trout. Food Cosmet. Toxicol. 13 (4), 441–443.
Creppy, E.E., 2002. Update of survey, regulation and toxic effects of mycotoxins in Europe. Toxicol. Lett. 127 (1–3), 19–28.
De Feijter, J.A., Benjamins, J., Veer, F.A., 1978. Ellipsometry as a tool to study the adsorption behavior of synthetic and biopolymers at the air–water interface. Biopolymers 17 (7), 1759–1772.
de los Santos Pereira, A., Kostina, N.Y., Bruns, M., Rodriguez-Emmenegger, C., Barner-Kowollik, C., 2015. Photo-triggered functionalization of hierarchically structured polymer brushes. Langmuir 31 (21), 5899–5907.
Deshpande, S., 2002. Fungal Toxins. Handbook of Food Toxicology. Marcel Decker, New York, pp. 387–456.
Dinçkaya, E., Kınık, Ö., Sezgintürk, M.K., Altuğ, Ç., Akkoca, A., 2011. Development of an impedimetric aflatoxin M1 biosensor based on a DNA probe and gold nanoparticles. Biosens. Bioelectron. 26 (9), 3806–3811.
Fallah, A.A., 2010. Assessment of aflatoxin M1 contamination in pasteurized and UHT milk marketed in central part of Iran. Food Chem. Toxicol. 48 (3), 988–991.
Galvano, F., Galofaro, V., Galvano, G., 1996. Occurrence and stability of aflatoxin M1 in milk and milk products: a worldwide review. J. Food Prot. 59 (10), 1079–1090.
Garden, S.R., Strachan, N.J.C., 2001. Novel colorimetric immunoassay for the detection of aflatoxin B1. Anal. Chim. Acta 444 (2), 187–191.
Homola, J., 2008. Surface plasmon resonance sensors for detection of chemical and biological species. Chem. Rev. 108 (2), 462–493.
Homola, J., Dostalek, J., Chen, S., Rasooly, A., Jiang, S., Yee, S.S., 2002. Spectral surface plasmon resonance biosensor for detection of staphylococcal enterotoxin B in milk. Int. J. Food Microbiol. 75 (1), 61–69.
Hu, W., Chen, H., Zhang, H., He, G., Li, X., Zhang, X., Liu, Y., Li, C.M., 2014. Sensitive detection of multiple mycotoxins by SPRi with gold nanoparticles as signal amplification tags. J. Colloid Interface Sci. 431, 71–76.
Kamkar, A., 2006. A study on the occurrence of aflatoxin M1 in Iranian Feta cheese. Food Control 17 (10), 768–775.
Kozma, P., Kozma, D., Nemeth, A., Jankovics, H., Kurunczi, S., Horvath, R., Vonderviszt, F., Fried, M., Petrik, P., 2011. In-depth characterization and computational 3D reconstruction of flagellar filament protein layer structure based on in situ spectroscopic ellipsometry measurements. Appl. Surf. Sci. 257 (16), 7160–7166.
Kuzmyn, A., Santos Pereira, A. de los, Pop-Georgievski, O., Bruns, M., Brynda, E., Rodriguez-Emmenegger, C., 2014. Exploiting end group functionalization for the design of antifouling bioactive brushes. Polym. Chem. 5 (13), 4124–4131.
LYON, F., 2014. IARC monographs on the evaluation of carcinogenic risks to humans.
Magliulo, M., Mirasoli, M., Simoni, P., Lelli, R., Portanti, O., Roda, A., 2005. Development and validation of an ultrasensitive chemiluminescent enzyme immunoassay for aflatoxin M1 in milk. J. Agric. Food Chem. 53 (9), 3300–3305.
Micheli, L., Grecco, R., Badea, M., Moscone, D., Palleschi, G., 2005. An electrochemical immunosensor for aflatoxin M1 determination in milk using screen-printed electrodes. Biosens. Bioelectron. 21 (4), 588–596.
Mitchell, J.S., Wu, Y., Cook, C.J., Main, L., 2005. Sensitivity enhancement of surface plasmon resonance biosensing of small molecules. Anal. Biochem. 343 (1), 125–135.
O'Shannessy, D.J., Brigham-Burke, M., Peck, K., 1992. Immobilization chemistries suitable for use in the BIAcore surface plasmon resonance detector. Anal. Biochem. 205 (1), 132–136.
Pei, S.C., Zhang, Y.Y., Eremin, S.A., Lee, W.J., 2009. Detection of aflatoxin M1 in milk products from China by ELISA using monoclonal antibodies. Food Control 20 (12), 1080–1085.
Polychronaki, N., West, R.M., Turner, P.C., Amra, H., Abdel-Wahhab, M., Mykkänen, H., El-Nezami, H., 2007. A longitudinal assessment of aflatoxin M1 excretion in breast milk of selected Egyptian mothers. Food Chem. Toxicol. 45 (7), 1210–1215.

Radoi, A., Targa, M., Prieto-Simon, B., Marty, J.L., 2008. Enzyme-Linked Immunosorbent Assay (ELISA) based on superparamagnetic nanoparticles for aflatoxin M1 detection. Talanta 77 (1), 138–143.
Regulation, H.A.T., 2006. Commission Regulation (EC) No 1154/2005.
Rodriguez-Emmenegger, C., Avramenko, O.A., Brynda, E., Skvor, J., Alles, A.B., 2011. Poly(HEMA) brushes emerging as a new platform for direct detection of food pathogen in milk samples. Biosens. Bioelectron. 26 (11), 4545–4551.
Rodriguez-Emmenegger, C., Brynda, E., Riedel, T., Houska, M., Šubr, V., Alles, A.B., Hasan, E., Gautrot, J.E., Huck, W.T.S., 2011. Polymer brushes showing non-fouling in blood plasma challenge the currently accepted design of protein resistant surfaces. Macromol. Rapid Commun. 32 (13), 952–957.
Rosmaninho, R., Santos, O., Nylander, T., Paulsson, M., Beuf, M., Benezech, T., Yiantsios, S., Andritsos, N., Karabelas, A., Rizzo, G., Müller-Steinhagen, H., Melo, L.F., 2007. Modified stainless steel surfaces targeted to reduce fouling – evaluation of fouling by milk components. J. Food Eng. 80 (4), 1176–1187.
Sapsford, K.E., Taitt, C.R., Fertig, S., Moore, M.H., Lassman, M.E., Maragos, C.M., Shriver-Lake, L.C., 2006. Indirect competitive immunoassay for detection of aflatoxin B1 in corn and nut products using the array biosensor. Biosens. Bioelectron. 21 (12), 2298–2305.
Sassahara, M., Pontes Netto, D., Yanaka, E.K., 2005. Aflatoxin occurrence in foodstuff supplied to dairy cattle and aflatoxin M1 in raw milk in the North of Paraná state. Food Chem. Toxicol. 43 (6), 981–984.
Szunerits, S., Spadavecchia, J., Boukherroub, R., 2014. Surface plasmon resonance: signal amplification using colloidal gold nanoparticles for enhanced sensitivity. Rev. Anal. Chem. 33 (3), 153–164.
Thirumala-Devi, K., Mayo, M.A., Hall, A.J., Craufurd, P.Q., Wheeler, T.R., Waliyar, F., Subrahmanyam, A., Reddy, D.V.R., 2002. Development and application of an indirect competitive enzyme-linked immunoassay for aflatoxin M1 in milk and milk-based confectionery. J. Agric. Food Chem. 50 (4), 933–937.
Trmcic-Cvitas, J., Hasan, E., Ramstedt, M., Li, X., Cooper, M.A., Abell, C., Huck, W.T.S., Gautrot, J.E., 2009. Biofunctionalized protein resistant oligo(ethylene glycol)-derived polymer brushes as selective immobilization and sensing platforms. Biomacromolecules 10 (10), 2885–2894.
Unusan, N., 2006. Occurrence of aflatoxin M1 in UHT milk in Turkey. Food Chem. Toxicol. 44 (11), 1897–1900.
US Food and Drug Administration, 1996. Sec. 527.400 Whole Milk, Low Fat Skim Milk-aflatoxin M1 (CPG 7106.210), FDA Compliance Policy Guides. FDA, Washington DC FDA, p. 219.
Vaisocherová, H., Yang, W., Zhang, Z., Cao, Z., Cheng, G., Piliarik, M., Homola, J., Jiang, S., 2008. Ultralow fouling and functionalizable surface chemistry based on a zwitterionic polymer enabling sensitive and specific protein detection in undiluted blood plasma. Anal. Chem. 80 (20), 7894–7901.
Vaisocherová, H., Zhang, Z., Yang, W., Cao, Z., Cheng, G., Taylor, A.D., Piliarik, M., Homola, J., Jiang, S., 2009. Functionalizable surface platform with reduced nonspecific protein adsorption from full blood plasma—material selection and protein immobilization optimization. Biosens. Bioelectron. 24 (7), 1924–1930.
Wang, Y., Dostalek, J., Knoll, W., 2011. Magnetic nanoparticle-enhanced biosensor based on grating-coupled surface plasmon resonance. Anal. Chem. 83 (16), 6202–6207.
Wang, Y., Dostálek, J., Knoll, W., 2009. Long range surface plasmon-enhanced fluorescence spectroscopy for the detection of aflatoxin M1 in milk. Biosens. Bioelectron. 24 (7), 2264–2267.
Zhang, X., Liu, L., Chen, X., Kuang, H., Song, S., Xu, C., 2013. Immunochromatographic strip development for ultrasensitive analysis of aflatoxin M1. Anal. Methods 5 (23), 6567–6571.